

Coner Frequencies and Q Values of P and S Waves by Simultaneous Inversion Technique

著者	Masuda Tetsu
雑誌名	The science reports of the Tohoku University. Fifth series, Tohoku geophysical journal
巻	31
号	3-4
ページ	101-125
発行年	1988-06
URL	http://hdl.handle.net/10097/45309

Corner Frequencies and Q Values of P and S Waves by Simultaneous Inversion Technique

TETSU MASUDA

Geophysical Institute, Faculty of Science
Tohoku University, Sendai 980, Japan

(Received May 9, 1988)

Abstract: The ratio of P to S wave corner frequency is investigated applying an objective technique of simultaneous inversion of source parameters and Q values on the observed spectra. Data used are the direct P and SH wave pulses of small earthquakes which occurred on the upper seismic plane in the northeastern part of Honshu, Japan. Focal depths of the earthquakes are about 50 km and epicentral distances to the station are about 15 km, so that P and S waves emerge to the station at nearly right angle as isolated pulses. The inversion method employed in the analysis, which assumes only the functional form of source spectrum and frequency dependence of Q value, separates the source and attenuation terms of observed spectra without any further presumptions. Q values are found almost constant, around 420 for P wave and 600 for S wave within the frequency band from 3 to 42 Hz, showing only a slight increase as frequency increases. The value of Q for S wave is about 1.4 times larger than that for P wave throughout the band.

It is shown that P wave corner frequencies are systematically larger than S wave corners. The average ratio is obtained as 1.32, and deviation from the average is small. In spite of varieties in amplitudes and in corner frequencies, the shapes of P wave spectra, as well as those of S wave spectra, are almost identical for all the earthquakes, though the average shape of P wave spectra is found different from that of S wave spectra. P wave source spectra decay in high frequencies as $f^{2.1}$, while SH wave spectra decay as $f^{1.7}$. The ratio 1.32 of P to SH wave corner frequency, and the difference in high frequency decay rate between P and SH waves, suggest circular sources with rupture velocity close to S wave velocity.

1. Introduction.

The difference of pulse widths in the time domain, or the difference of corner frequencies in the frequency domain, between P and S waves is an important problem in theoretical and observational seismology. This problem has come to be argued in detail through the series of theoretical studies on seismic source (Ben-Menahem, 1962; Haskell, 1964; Hirasawa and Stauder, 1965; Savage, 1966a; Brune, 1970; Trifunac, 1972; Mernar *et al.*, 1973; Sato and Hirasawa, 1973; Madariaga, 1976; Masuda *et al.*, 1977). Along with theoretical works, observational approach to the problem has also been developed extensively. Hanks and Wyss (1972) made spectral analyses of three large, shallow earthquakes, and their measurements showed that P wave corners are higher than S wave corners. Molnar and Wyss (1972) also showed higher corner frequencies of P wave spectra than those of S wave spectra for large shallow earthquakes in the Tonga-Kermadec region. Trifunac (1972) and Molnar *et al.* (1973) analysed many of the aftershocks of the 1971 San Fernando, California earthquake. The corner frequency

shift was also observed for most of the aftershocks, the ratios of P to S wave corners being as much as about a factor of 3 for some of the earthquakes. Masuda and Takagi (1978) found that corner frequencies of P waves are 1.4 times higher on the average than those of S waves for small earthquakes at focal depths of 30 km to 50 km in the northeastern part of Honshu, Japan. Fletcher (1980) observed P wave corner frequencies 1.7 times higher than S wave corner frequencies for Oroville, California aftershocks. Many of observations have shown longer pulse widths, or lower corner frequencies, of S waves than of P waves for small to large earthquakes. There were, however, a few reports that P wave corner frequency is not higher than S wave corner frequency. Bakun *et al.* (1976) showed higher corner frequencies of S wave spectra for small earthquakes in central California. No systematical shift between P and S wave corners were reported for small earthquakes in the Geysers geothermal area in California (Peppin and Bufe, 1980). Hanks (1981) reviewed the observations of corner frequency shift to discuss its potential for discrimination of seismic sources.

As reviewed above, P wave corner frequency is higher than S wave corner frequency for the majority of earthquakes despite the region, size, and depth of earthquakes. The corner frequency shift has been accepted as an observational fact. This stimulated theoretical derivations associated explicitly with corner frequency shift (Savage, 1972, 1974; Molnar *et al.*, 1973; Dahlen, 1974), and consequently established a refined viewpoint as for interpretation of corner frequency (Savage, 1974; Silver, 1983). There are, nevertheless, still a few problems left to be discussed with regard to corner frequency measurement as well as to interpretation of corner frequency shift. The problems in previous measurements of corner frequency are namely the quality of wave form data, separation of attenuation effects from the spectra, and method of measuring corners of the spectra. Each of them is reviewed in some detail in the followings.

First, the quality of wave form data in the literature is reexamined from a viewpoint of distortion of observed pulses. Some of the previous works analysed shallow local earthquakes whose epicentral distances to stations were long compared with focal depths (e.g., Thatcher and Hanks, 1973; Fletcher, 1980; Peppin and Bufe, 1980; McGarr *et al.*, 1981; Scherbaum and Stoll, 1983). The first arrivals are considered likely to be head waves or diving waves which travelled a long horizontal distance. In these cases, there are mainly two problems in analysing the P or S wave pulse. Firstly, the spectral characteristic of observed pulse is sensitive to the velocity structure around horizontal boundary of discontinuity along the path. A detailed structure around the boundary is not always obtained, therefore, it is not an easy task to adequately correct for propagation effect. Secondly, the tail of P or S wave pulse is mostly buried in wave trains of large amplitude later phases due to reflections or scatterings. Inevitably a time window includes not only P or S wave pulse but also other later arrivals. The reflected or scattered waves generally have different source effect and experience different propagation effect from the first arrival of P or S wave pulse. The spectrum calculated for a wave train is a mixture of many phases with different spectra. It is thus difficult to purely extract the spectral property of P or S wave pulse. The pulse to be analysed is

direct P or S wave pulse isolated from multiple later phases, for which it is possible to unambiguously deduce source spectrum of radiated pulse on the focal sphere. It is necessary to investigate corner frequency shift for isolated P and S wave pulses free from contaminations by later phases.

Second, some problems in correcting for attenuation effects are described. Observed displacement spectra are the product of source term and attenuation effect. For a medium where the attenuation factor Q is almost independent of frequency, high frequency components of spectrum are more effectively attenuated than low frequency components, which distorts the amplitude spectrum. The corner frequency measurements are thus influenced by the manner in which corrections for attenuation effects are made. In some cases, corrections for attenuation have been made by simply assuming Q values (e.g., Fletcher, 1980; Bungum *et al.*, 1982). Other studies have made corrections by applying Q values obtained in independent works of the concerned area (e.g., Thatcher and Hanks, 1973; Marion and Long, 1980). In these cases, however, the value used in the analysis is not the very value of Q along a particular path from earthquake. Moreover, Q values are not always obtained for both P and S waves, but the value of Q for P or S wave is calculated from the value of the other assuming the ratio of Q value for P to S wave (e.g., Marion and Long, 1980). The ratio of Q value for P to S wave is not yet solved in the frequency band appropriate for spectral study of small earthquakes. The attenuation effect is serious in an analysis of small earthquake even for a short hypocentral distance, since to frequency band of spectrum ranges to fairly high frequencies. Inadequate correction may lead to a large error in estimate of corner frequency, and may thus lead to considerably erroneous estimate of the corner frequency ratio.

Finally, the most important point which relates to errors in corner frequency is, as a matter of course, the method to pick up the position of corner of amplitude spectrum. Conventional methods of estimating the corner have been owing to visual fitting of a model spectrum to the observed one. A familiar technique of picking up the corner is to fit two segments of straight lines respectively to low and to high frequency regions of the bilogarithmic plot of spectra (Hanks and Wyss, 1972; Thatcher and Hanks, 1973; McGarr *et al.*, 1981; Scherbaum and Stoll, 1983; Hasegawa, 1983). The corner frequency is defined as the intersection of the two segments. Another model spectrum is a Brune's spectrum of simple form (Spottiswoode and McGarr, 1975; Marion and Long, 1980), though the high frequency fall-off may have been left misfit. Those procedures of determining corner frequency by visual measurement, being not based on a mathematical standard, are quite subjective and dependent on individual complexities of spectra. It is difficult to estimate the certainty of measurements on a universal standpoint. The ambiguity of estimates arises from measurement procedure itself, and thus a definite conclusion cannot be drawn on quantitative arguments of corner frequency. This is a reason why the previous discussion was restricted on only qualitatively which of P or S wave corner frequency is higher, but was not extended on quantitatively what amount P or S wave corner frequency is higher than the other.

In the present study, corner frequencies of P and SH wave pulses are measured under an ideal condition where each of the problems described above is removed. The method employed here, an objective technique of simultaneous inversion of source parameters and Q values (Masuda and Suzuki, 1982), separates the effect of inelastic attenuation from the observed spectra, and thus exposes the average shapes of source spectra of P and S waves. Corner frequencies of P and S waves and their certainties are estimated on the same basis for all of the earthquakes, and high frequency decay rates of source spectra are obtained as well. Based on accurate measurements, the difference of spectral characteristics between P and S waves and its implications are discussed in relation to source theory.

2. Data

The microearthquake observation network of Tohoku University has been locating small earthquakes in shallow parts of the crust and along the two intermediate depth seismic planes in and around the northeastern part of Honshu, Japan, as well as in the southern part of Hokkaido (Umino and Hasegawa, 1982; Umino *et al.*, 1984). The precise location routine have revealed several spots of small dimensions where seismic activities are constantly high. Among these, the one which is located a slightly off the Pacific coast of the Iwate Prefecture and at the depth of about 50 km on the upper seismic plane is selected for the present study of investigating the corner frequency shift. The station MYK of the microearthquake observation network of Tohoku University is located at short distances from the high activity spot of earthquakes studied in the present study. Fig.1 plots the station MYK to show relative location to the hypocenters.

A temporal observation was carried out during a period from December 1978 to February 1980. Several tens of earthquakes occurred in the high activity spot during the period of temporal observation. P wave pulses of 34 earthquakes, and S wave pulses of 14 earthquakes were available. S wave motions of 20 earthquakes were unfortunately out of scale. The simultaneous inversion method proposed by Masuda and Suzuki (1982) and employed here requires a number of earthquakes not too small for an accurate estimation of source parameters and Q value. Numerical tests of the method indicate that a number about 10 of earthquakes is quite sufficient (Masuda and Suzuki, 1982). It is preferable, however, to include as many of earthquakes as possible for a good result. Thus P wave pulses of all 34 earthquakes, and S wave pulses of 14 earthquakes are analysed.

Hypocenters and magnitudes of the earthquakes are determined by the Observation Center for Earthquake Prediction, Tohoku University. Hypocentral parameters of the earthquakes are given in Table 1. The magnitudes of earthquakes, which are determined according to the total duration of signal, range from 0.9 to 3.3. The earthquakes are located at depths between 43 and 53 km, mostly around 47 to 49 km, on the upper seismic plane. The epicentral distances to MYK are about 14 km for most of the earthquakes, and are less than 25 km at most. Travel times of P and S waves from

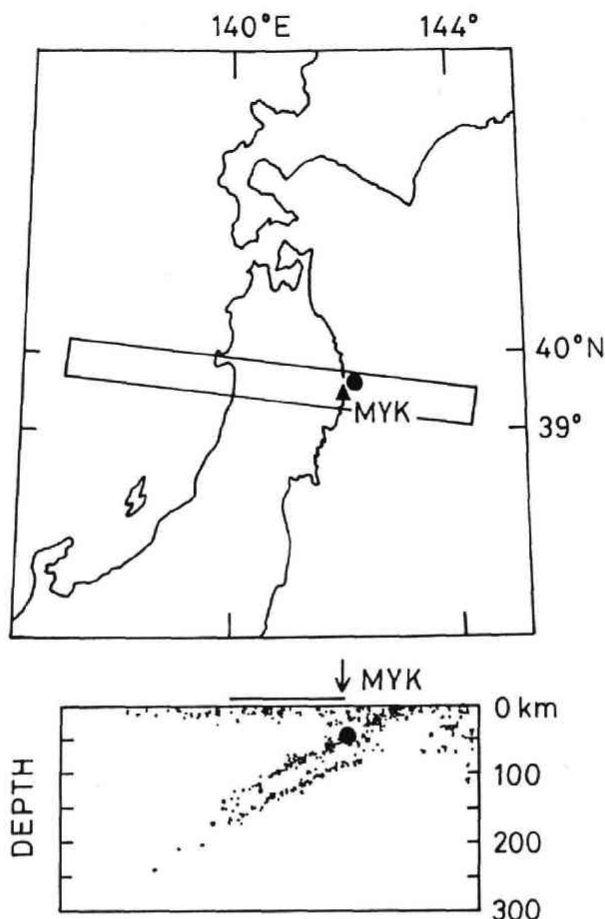


Fig. 1 A map and a cross-section showing the location of station MYK and the hypocenters of earthquakes analysed in this study. Projected in the cross-section is the seismicity within the strip shown in the map. The earthquakes occurred within a small volume which is located 15 km northeast of MYK and 50 km deep. Cross-section of microearthquake hypocenters is after Umino and Hasegawa (1982).

these earthquakes to MYK are about 7.2 to 8.1 seconds and about 12.6 to 13.6 seconds, respectively. Since the station MYK is located at short epicentral distance compared with focal depth of the earthquakes, the focal depth is quite well constrained as well as the epicentral location. The location errors are estimated as less than 3 km in all of the three coordinates.

The focal mechanisms of small earthquakes along the intermediate depth seismic planes were studied by Umino and Hasegawa (1982) and Umino *et al.* (1984). The composite mechanisms of earthquakes which occurred at depths around 50 km on the upper seismic plane were obtained in these studies, though there was no single earthquake for which the focal mechanism was determined. The mechanism solution shows

Table 1. List of hypocentral parameters of the earthquakes

<i>no</i>	<i>date</i>	<i>time</i>	<i>lat</i>	<i>lon</i>	<i>dep</i>	<i>mag</i>	<i>del</i>	<i>t_p</i>	<i>t_s</i>
1	1978 12 31	6:04	39.631	142.119	48.4	2.5	12.6	7.5	—
2	1979 1 1	5:58	39.654	142.138	46.6	3.1	15.2	7.4	—
3	1979 1 5	7:21	39.643	142.127	48.1	2.4	13.8	7.5	12.8
4	1979 2 9	17:19	39.638	142.153	48.3	2.0	15.6	7.6	13.0
5	1979 3 1	0:10	39.646	142.157	48.7	2.1	16.3	7.7	13.1
6	1979 3 4	8:29	39.745	142.186	46.8	1.9	24.5	7.9	13.6
7	1979 3 4	11:06	39.730	142.169	46.8	1.8	22.3	7.8	13.1
8	1979 3 20	7:30	39.685	142.146	47.7	2.9	17.6	7.6	—
9	1979 4 11	2:56	39.696	142.195	49.8	3.2	21.7	8.1	—
10	1979 4 12	4:19	39.672	142.153	46.7	2.3	17.3	7.5	—
11	1979 4 12	4:19	39.675	142.147	47.6	2.8	17.2	7.6	—
12	1979 4 18	15:14	39.712	142.142	47.1	1.7	19.3	7.6	13.1
13	1979 4 30	0:49	39.672	142.134	48.5	2.2	15.9	7.6	13.1
14	1979 5 2	19:36	39.694	142.130	47.2	2.4	17.2	7.5	12.9
15	1979 5 11	13:00	39.638	142.128	48.2	3.1	13.6	7.5	—
16	1979 6 4	16:26	39.630	142.136	47.1	1.8	14.0	7.4	—
17	1979 6 11	0:34	39.640	142.140	49.1	2.3	14.7	7.6	—
18	1979 6 25	8:14	39.639	142.133	49.3	2.4	14.1	7.6	—
19	1979 6 27	5:21	39.630	142.131	47.2	1.4	13.5	7.4	—
20	1979 7 8	9:16	39.641	142.135	48.2	2.2	14.3	7.5	12.9
21	1979 7 8	10:50	39.673	142.144	48.2	3.0	16.7	7.6	—
22	1979 7 8	16:51	39.709	142.120	44.8	.9	17.7	7.3	—
23	1979 7 12	2:26	39.635	142.111	46.2	1.1	12.2	7.2	—
24	1979 7 19	4:09	39.687	142.135	46.7	1.5	17.0	7.5	12.8
25	1979 7 25	2:28	39.619	142.120	47.2	1.5	12.3	7.3	—
26	1979 7 29	2:05	39.605	142.151	49.5	3.2	14.6	7.7	—
27	1979 7 30	6:14	39.621	142.134	50.7	2.8	13.5	7.8	—
28	1979 8 1	1:03	39.631	142.137	49.4	3.3	14.1	7.7	—
29	1979 8 1	17:53	39.686	142.133	46.4	1.4	16.8	7.4	12.7
30	1979 8 3	6:23	39.635	142.152	48.9	1.8	15.4	7.6	13.1
31	1979 8 5	3:50	39.734	142.155	42.8	1.6	21.8	7.3	—
32	1979 8 10	4:52	39.622	142.162	46.3	2.0	15.9	7.3	12.6
33	1979 8 25	4:04	39.640	142.136	49.6	2.1	14.3	7.7	13.2
34	1979 8 26	12:00	39.623	142.161	52.8	2.7	15.8	8.1	—

lat: latitude in degree north; *lon*: longitude in degree east; *dep*: depth in km; *mag*: magnitude; *del*: epicentral distance in km; *t_p*: *P* wave travel time in sec; *t_s*: *S* wave travel time in sec.

a reverse faulting for these earthquakes. One of the *P* wave nodal planes has a strike of 120 to 160 degrees west of north, a dip angle of 20 to 40 degrees, and slip angle of 60 to 120 degrees counterclockwise from the strike. Faulting on this plane is consistent with the subducting motion of the Pacific plate, so that this plane is reasonably regarded as the fault plane. This is the typical solution for earthquakes which occur at depths

around 50 km on the upper seismic plane and along the Pacific coast of the northeastern Honshu, Japan. The radiation pattern coefficients are calculated as 0.5 to 0.9 at MYK both for P and SH waves, so that good signal to noise ratios are obtained both for P and SH wave pulses.

During the temporal observation, an electro-magnetic seismometer with three components were installed in a deep tunnel where the ground noise level is quite low. The natural frequency of pendulum is 4.5 Hz, which is suitable for high corner frequencies expected for the earthquakes. Two horizontal components, polarized to north-south and east-west directions, have smaller magnification than vertical component by a factor of 5, expecting larger signal amplitudes for S waves. Seismic signals were picked up by the seismometer, A/D converted, and delayed for about 3 seconds through a digital memory. The resolution of A/D converter was 8 bit, and sampling rate was 700 Hz. Signals were then D/A converted, and finally were recorded on an FM data recorder. The overall frequency response of the observation system is flat to the ground velocity between 6 and 70 Hz. The temporal observation yielded seismic records for a frequency band from 3 to 70 Hz, wide enough for spectral study of small earthquakes. Typical seismograms on three components are given in Fig. 2. Impulsive arrivals of isolated P and S wave pulses are obvious in the figure. Seismograms of other earthquakes are more or less of the same characteristic with those shown in the

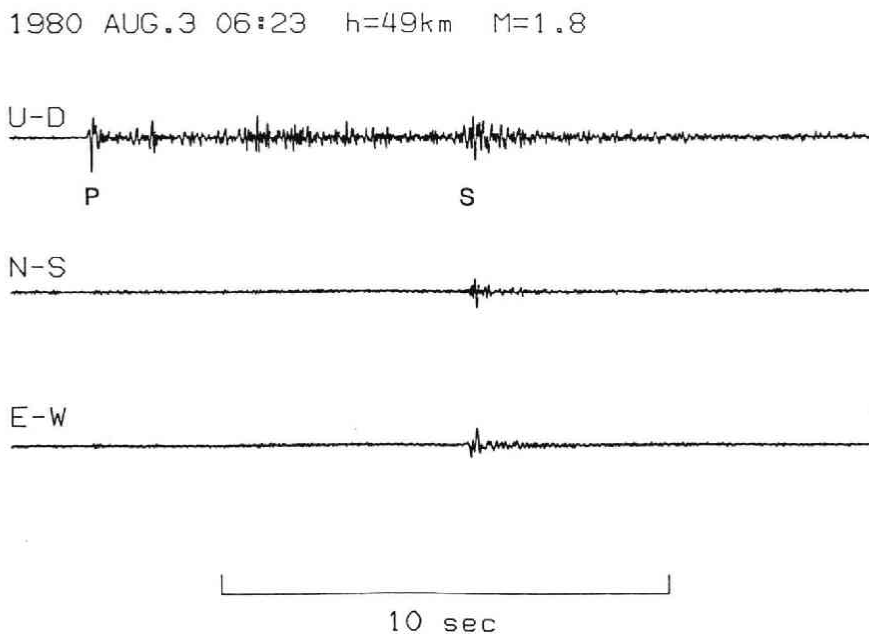


Fig. 2 Three-component seismogram showing impulsive arrivals of isolated P and S waves from a magnitude 1.8 earthquake at the depth of 49 km. The magnification gains of horizontal components are 5 times less than that of vertical component.

figure. Direct P and S wave pulses from these earthquakes arrive at the station MYK with nearly vertical emergent angle, so that they are isolated from later arrivals and not contaminated by scattered waves. This is a very preferable situation to the study of corner frequency shift.

In this study, P wave pulses on vertical component, and SH wave pulses synthesized by appropriate rotation of the two horizontal components are analysed. Smoothed spectra of pulses are estimated from outputs of 1-pole Butterworth-type band-pass filters at 10 frequencies equally spaced in logarithmic scale from 3.2 to 42 Hz. The quality factor of filter is chosen as 10. The maximum peak to peak amplitude is measured within 0.5 seconds from the onset of P or S wave pulse, and is used to evaluate Fourier spectrum. The effective pass band of filter, though it is proportional to center frequency, is narrow enough that Fourier amplitudes of input signal are regarded as constant within the pass band. Thus, the output amplitude of filter is practically related only to Fourier spectral component at the center frequency of filter.

It is unfortunately not straightforward, however, to convert filter outputs to Fourier spectral components, since the relationship between amplitudes of filter output and Fourier components depends on both amplitude and phase characteristics of input signal. At low frequencies, where amplitude spectrum of seismic signal is flat and phase of spectrum is regarded as constant within the pass band of filter, the following equation is valid to evaluate Fourier spectral amplitude from filter output ;

$$|\tilde{v}(f_o)| = \frac{g_{\max}/2}{2\pi f_o/Q_f} \quad (1)$$

g_{\max} is the maximum peak to peak amplitude of filter output. f_o is the center frequency, and Q_f the quality factor of band-pass filter. At high frequencies beyond the corner of spectrum, however, phase of spectrum changes by large amount within the linear range of pass band of filter though amplitude of spectrum may remain nearly constant. In this case, an alternative equation relates filter output to Fourier amplitude as ;

$$|\tilde{v}(f_o)| = \frac{g_{\max}/2}{\sqrt{2\pi f_o/Q_f \tau_d}}, \quad (2)$$

where τ_d is the duration for which filter output retains an amplitude close to its maximum. Derivation of equations (1) and (2) is given in Appendix. Relationships between filter outputs and Fourier spectra were discussed in detail in Masuda (1982). Following Masuda (1982), Fourier spectrum is approximated at low frequencies by the value according to equation (2) until it gives a smaller value than due to equation (1). At higher frequencies, the relation (1) is used to evaluate Fourier spectrum from filter outputs. Saito and Masuda (1981) also evaluated spectra in a similar manner.

The estimated Fourier components of seismometer outputs $|\tilde{v}(f_o)|$ are then corrected for instrument response and free surface effect. The correction for free surface effect on P wave pulses are made according to emergent angle of the ray calculated for the same velocity structure as used in locating hypocenters by the Observation Center for Earthquake Prediction, Tohoku University. The effect of free surface on SH wave is

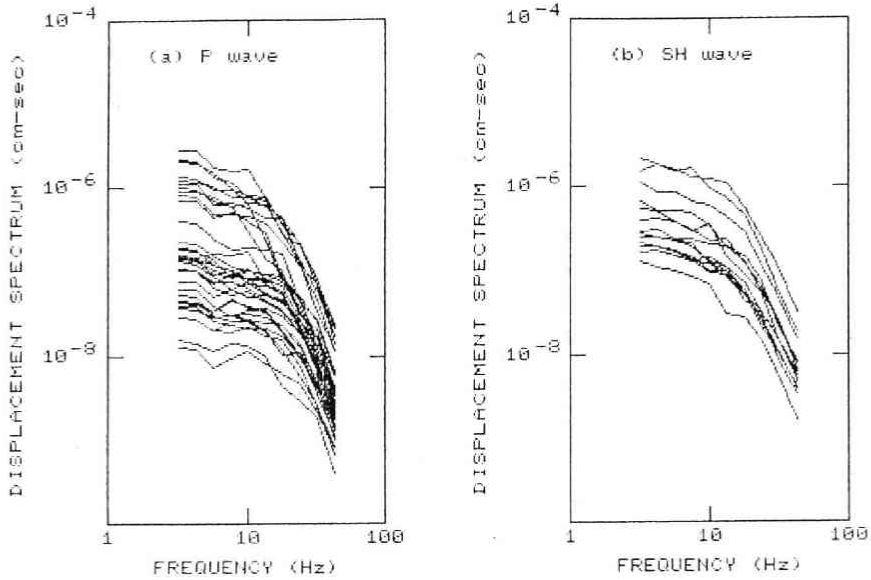


Fig. 3 Observed displacement spectra of (a) P waves and (b) SH waves plotted together to show their similarity in shape despite varieties in low frequency amplitude and in spectral corner.

merely to double the amplitudes. Displacement spectra $|\tilde{u}(f_o)|$ of P and SH waves are thus obtained, and are plotted in Fig. 3(a) and Fig. 3(b), respectively. From these spectra, low frequency amplitude, corner frequency, high frequency decay rate, and Q value are derived by means of simultaneous inversion technique proposed by Masuda and Suzuki (1982).

3. Method of analysis

The present study used the inversion method developed by Masuda and Suzuki (1982) which extracts source parameters and Q value simultaneously from amplitude spectra of local earthquakes in a small volume. Their method is briefly reviewed in the followings. Observed displacement spectrum consists of a source term and a term due to inelastic attenuation, and is written as,

$$|\tilde{u}(f)| = |\tilde{u}_s(f)| \exp(-\pi f t_r / Q), \quad (3)$$

where $|\tilde{u}_s(f)|$ is the source spectrum, t_r the travel time, and Q is the inelastic attenuation factor. Displacement amplitude spectrum $|\tilde{u}_s(f)|$ at the source is assumed to be of the form,

$$|\tilde{u}_s(f)| = \frac{\tilde{u}_o}{[1 + (f/f_c)^a]^{\gamma/a}}, \quad (4)$$

where \tilde{u}_o is the low frequency amplitude, and f_c the corner frequency. γ determines high frequency fall-off, and a is a positive constant according to which the behaviour of

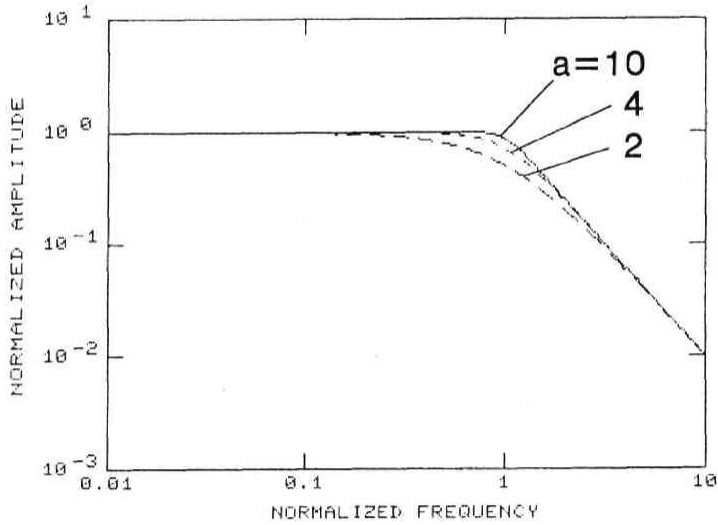


Fig. 4 Functional forms of source spectrum expressed in equation (4) for various values of a with γ fixed at 2. Solid curve is for $a=10$, short dashed for $a=4$, and long dashed for $a=2$. The curve for $a=2$ is identical to the source model by Brune (1970). A choice of a around 4 to 10 provides a good approximation of the smoothed shape of most of the source models proposed by Sato and Hirasawa (1973), Madariaga (1976), and Masuda *et al.* (1977).

spectrum near the corner varies. Some typical shapes of spectrum expressed as equation (4) are shown in Fig. 4 for various values of a and a fixed value of $\gamma=2$. It is seen that the corner of spectrum is sharper, but that the shapes of spectrum are not distinguishable for larger values of a . Most of theoretical spectra are represented by equation (4) with appropriate values of γ and a , though the assumed form has only two degrees of freedom regarding the shape of spectrum, while the shape of theoretical spectra of various models may be more complicated. The model proposed by Brune (1970) is identical with the case $\gamma=2$ and $a=2$. Smoothed amplitude spectra given by Sato and Hirasawa (1973), Madariaga (1976), and Masuda *et al.* (1977) are approximated by equation (4) with $\gamma=2$ and $a=4$ to 10. It is thus quite reasonable but is not a strong restriction to the analysis to assume the shape of source spectrum as expressed in equation (4). The value of Q in equation (3) may be dependent on frequency, and is assumed to be proportional to some power of frequency,

$$Q = q \cdot f^n, \quad (5)$$

as is suggested in many studies of coda waves (Aki and Chouet, 1975; Rautian and Khalturnin, 1978; Sato, 1986; Butler *et al.*, 1987; Matsumoto, 1987).

The model spectrum (3) with source term (4) and frequency dependent Q (5) is compared with the observed spectrum. P and SH wave data are separately analysed. Since the hypocenters are concentrated in a small volume and ray paths from earthquakes to the station MYK are almost identical, all earthquakes share the same effect

by inelastic attenuation. Therefore, the values of q and n in equation (5) are common for each set of P or S wave spectra. As the spectral shapes of all earthquakes are similar for each of P or SH wave (Fig. 3), common values of γ and a in equation (4) are also applied to all of the earthquakes for each of P or SH wave spectra. Unknown parameters in each of P or S wave analysis are thus low frequency amplitude \tilde{u}_0 and corner frequency f_c of each earthquake, parameters of spectral shapes γ and a and parameters of inelastic attenuation q and n common for all the earthquakes.

The errors in observed spectra are supposed to enter as some fraction of spectral amplitudes, but not as absolute magnitudes. Thus the least squares inversion searches the solution parameters which minimize the sum of squared residuals in logarithmic quantities at all frequencies and for all earthquakes. Since the normal equations for parameters are not linear, tentative solutions are initially necessary to find adjustments for parameters. Initial values of the parameters γ and a are put as 2.0 and 5.0 both in P and SH wave analyses. Initial guesses of low frequency amplitudes and corner frequencies are given by visual measurements from each spectrum. The values of q and n for P and SH waves are both initially chosen as 500 and 0.5 referring to the results by Umino and Hasegawa (1984) and Matsumoto (1987). The damped least squares technique is employed to obtain stable solutions to nonlinear inversion problems. In this study, damping constants are 0.1 for all parameters but a parameters a , for which heavier damping is applied with a constant equal to 1.0. This is because only a poor resolution is expected with regard to parameter a for spectra with sharp corners. The solutions

Table 2. Results of inversion

frequency dependent Q		
	P wave analysis	S wave analysis
initial data variance	1.067	0.845
final data variance	0.037	0.019
minimum of \tilde{u}_0 (cm-sec)	1.6×10^{-6}	1.5×10^{-7}
maximum of u_0 (cm-sec)	3.0×10^{-6}	2.7×10^{-6}
minimum of f_c (Hz)	5.9	12.9
maximum of f_c (Hz)	29.4	20.3
value of γ	2.06 ± 0.18	1.74 ± 0.32
value of a	11.2 ± 4.9	4.30 ± 1.89
value of q	360 ± 110	420 ± 230
value of n	0.050 ± 0.091	0.114 ± 0.182
constant Q		
	P wave analysis	S wave analysis
final data variance	0.037	0.019
value of γ	1.98 ± 0.13	1.63 ± 0.22
value of a	11.3 ± 5.1	4.30 ± 2.12
value of Q	420 ± 30	610 ± 120

are improved through iterative steps until data variance no more decreases.

4. Results

The final solutions are obtained at the sixth iteration step in each of P or SH wave analysis. The results are listed in Table 2 and Table 3. Data variances are reduced

Table 3. List of source parameters

<i>no</i>	<i>date</i>	<i>time</i>	$\bar{u}_0 (P)$	$f_c (P)$	$\bar{u}_0 (S)$	$f_c (S)$
1	1978 12 31	6:04	2.25 E-07	20.4	—	—
2	1979 1 1	5:58	8.28 E-07	17.2	—	—
3	1979 1 5	7:21	1.17 E-07	21.9	1.31 E-06	15.6
4	1979 2 9	17:19	1.72 E-07	15.7	8.05 E-07	14.4
5	1979 3 1	0:10	5.61 E-08	24.2	3.28 E-07	17.1
6	1979 3 4	8:29	6.33 E-07	21.9	2.55 E-07	18.2
7	1979 3 4	11:06	6.15 E-08	19.6	2.72 E-07	17.5
8	1979 3 20	7:30	1.07 E-06	8.9	—	—
9	1979 4 11	2:56	3.02 E-06	11.4	—	—
10	1979 4 12	4:19	3.92 E-07	18.3	—	—
11	1979 4 12	4:19	1.42 E-06	15.5	—	—
12	1979 4 18	15:14	1.07 E-07	22.8	6.61 E-07	13.0
13	1979 4 30	0:49	2.02 E-07	21.3	2.69 E-06	16.5
14	1979 5 2	19:36	2.24 E-07	19.4	2.46 E-06	12.9
15	1979 5 11	13:00	1.12 E-06	18.8	—	—
16	1979 6 4	16:26	1.61 E-07	16.3	—	—
17	1979 6 11	0:34	1.80 E-07	15.6	—	—
18	1979 6 25	8:14	1.75 E-07	19.9	—	—
19	1979 6 27	5:21	4.37 E-08	21.8	—	—
20	1979 7 8	9:16	1.33 E-07	17.9	3.42 E-07	14.4
21	1979 7 8	10:50	2.44 E-06	5.9	—	—
22	1979 7 8	16:51	1.56 E-08	29.4	—	—
23	1979 7 12	2:26	4.62 E-08	16.9	—	—
24	1979 7 19	4:09	3.60 E-08	20.1	2.41 E-07	16.9
25	1979 7 25	2:28	6.24 E-08	21.0	—	—
26	1979 7 29	2:05	1.53 E-06	17.2	—	—
27	1979 7 30	6:14	7.79 E-07	12.5	—	—
28	1979 8 1	1:03	2.00 E-06	14.2	—	—
29	1979 8 1	17:53	1.90 E-08	20.1	1.50 E-07	14.7
30	1979 8 3	6:23	1.04 E-07	21.1	5.69 E-07	17.9
31	1979 8 5	3:50	3.71 E-08	25.8	—	—
32	1979 8 10	4:52	5.81 E-08	29.1	2.73 E-07	20.1
33	1979 8 25	4:04	1.24 E-07	26.1	4.43 E-07	20.3
34	1979 8 26	12:00	1.18 E-06	15.5	—	—

$\bar{u}_0 (P)$ and $\bar{u}_0 (S)$: low frequency amplitude of P and S wave in cm-sec, respectively ;
 $f_c (P)$ and $f_c (S)$: corner frequency of P and S wave in Hz, respectively.

from 1.067 to 0.037 in the P wave analysis, and from 0.845 to 0.019 in the SH wave analysis. In order to examine the stability of solutions, numbers of inversion procedures are carried out with different damping constants and from different initial values of parameters. It is found that almost the same final solutions and data variance are attained in all runs of inversion for each of P or S wave analysis. It has also been shown in Masuda and Suzuki (1982) that final solutions are independent of initial guesses of solution parameters, and that damping constants have no influence on values of final solutions but only on convergence speed of solutions.

The source parameters, low frequency amplitude and corner frequency of spectrum, are accurately estimated within a few percent of errors for both P and SH waves. The relationships between low frequency amplitude and corner frequency are shown in Fig. 5(a) for P waves and Fig. 5(b) for SH waves, respectively. Low frequency amplitudes of spectra range from 1.6×10^{-8} to 3.0×10^{-6} cm-sec for P wave, and from 1.5×10^{-7} to 2.7×10^{-6} cm-sec for SH waves. Corner frequencies of P waves are obtained as 5.9 Hz at lowest and as 29 Hz at highest for all of 34 earthquakes. For 14 earthquakes for which P and SH waves are analysed, P wave corner frequencies range from 15.7 to 29.1 Hz, and SH wave corner frequencies from 12.9 to 20.3 Hz. It is seen in the figure that corner frequencies do not decrease so much as low frequency amplitudes increase. The low frequency amplitude is inversely proportional to the sixth to tenth power of corner frequency both of P and SH waves. The relationship between low frequency amplitude and corner frequency is different from the one established for large earthquakes. Similar relationships are found for small earthquakes in many regions (e.g., Masuda and Takagi, 1978; Masuda and Suzuki, 1982; Hasegawa, 1983)

A comparison is made between low frequency amplitudes and duration magnitudes

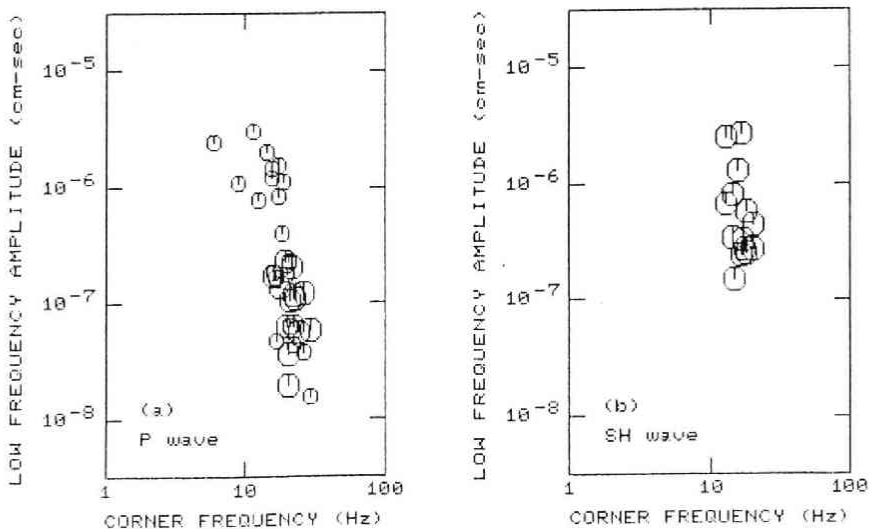


Fig. 5 Low frequency amplitude versus corner frequency for (a) P waves and (b) SH waves. The corner frequency shift is obvious in these figures.

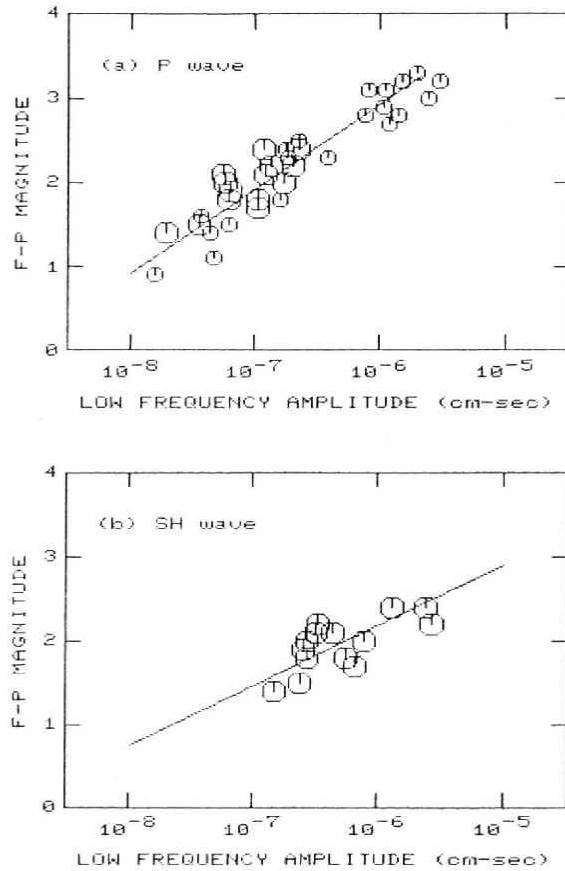


Fig. 6 Low frequency amplitude of spectrum versus magnitude for (a) *P* waves and (b) *SH* waves. Magnitudes of earthquakes are determined according to the total duration of signal. Data show a linear correlation between magnitude and logarithm of low frequency amplitude. The regression line is indicated in the figure of each of *P* and *SH* wave data.

of the earthquakes for a check of reliability of solutions. Fig. 6(a) shows the relation for *P* wave data, and Fig. 6(b) for *SH* wave data. Small symbols in *P* wave data diagram represent the earthquakes for which no *SH* wave data are present. The regression lines of magnitude against logarithm of low frequency amplitude are also shown in the figures. The slope is found to be 1.0 for *P* wave data, while for *SH* wave data a smaller value of 0.7 is obtained. Since the number of *SH* wave data is not sufficient to derive a definite relationship between magnitude and low frequency amplitude, the same slope 1.0 as for *P* wave data seem to equally well explain the relationship for *SH* wave data. Similar values of slope have been obtained for earthquakes in many regions (Masuda and Takagi, 1978; Peppin and Bufe, 1980; Bungum *et al.*, 1982; Hasegawa, 1983; Scherbaum and Stoll, 1983). The scatter of data from regression line is small enough to assure that logarithm of low frequency amplitude is proportional to duration magnitude

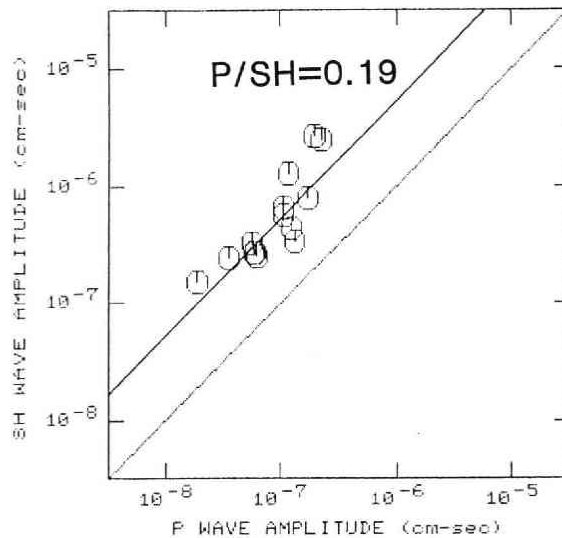


Fig. 7 Relationship between low frequency amplitudes of P and SH wave spectra. The average ratio is obtained as 0.19. Scatter of the data is as small as a factor of 2.

of earthquake. The total duration of signal is generally considered not sensitive to such effects as geometrical spreading, inelastic attenuation along the path, structure at the source and at station site, radiation pattern, so that duration magnitude is a good measure of relative magnitude of earthquake. Thus it is concluded that the technique used in this study was successful in consistently estimating low frequency amplitudes of spectra.

Another check is made for the consistency of relative estimates of low frequency amplitudes of P and SH wave spectra. Fig. 7 compares low frequency amplitudes of P and SH wave spectra for 14 earthquakes. The average ratio of low frequency amplitude of P to SH waves is about 0.19. The ratio of P to S wave velocity is about 1.7 to 1.8 around the crust and upper most mantle. Since low frequency amplitude ratio of P to SH wave spectra is inversely proportional to the cube of the velocity ratio, the amplitude ratio of 0.19 obtained for the earthquakes implies that the radiation pattern coefficients of P and SH waves are nearly identical. This is in good agreement with composite mechanism solutions for the earthquakes. The scatter of data from straight line with slope 1 shown in the figure is only less than a factor of 2 or so, which again suggests that the inversion method consistently determines low frequency amplitudes of P and SH wave spectra for all the earthquakes.

Fig. 5 shows that the relationships between low frequency amplitude and corner frequency of P and SH waves are almost identical for earthquakes for which both P and SH wave data are present. It is also seen in Fig. 5 that corner frequencies of P waves are systematically higher than those of SH waves. A graphical measurement from the figure may give the average ratio of P to SH wave corner frequencies of about 1.3. Fig.

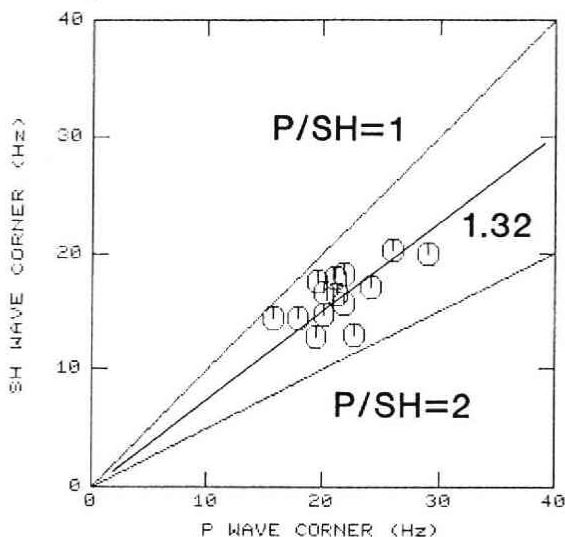


Fig. 8 Comparison of corner frequencies between P and SH waves. The ratio of P wave to SH wave corner frequency is always greater than 1 but smaller than 2. The average ratio is 1.32, and deviation from the average is small.

8 illuminates a direct comparison of corner frequencies between P and SH waves for each of 14 earthquakes. Solid lines with slope 1 and 0.5 indicate ratios of P to SH wave corner frequency equal to 1 and 2, respectively. The ratio is always greater than unity, and is less than 1.8 for these earthquakes. The average ratio is obtained as 1.32, which is indicated by a straight line in the figure. Scatter of each value of ratio from the average is fairly small.

Other source parameters, γ and a which determines the shape of spectra, are obtained as 2.06 ± 0.18 and 11.2 ± 4.9 for P wave spectra, and 1.74 ± 0.32 and 4.30 ± 1.89 for SH wave spectra, respectively. Fig. 9(a) shows P wave source displacement spectra of 34 earthquakes, and Fig. 9(b) shows SH wave source displacement spectra of 14 earthquakes. In these figures, spectral amplitude normalized by the low frequency amplitude is plotted against frequency normalized by the corner frequency of each earthquake. The average spectral shape may be depicted in the figure. Similarity of all spectral shapes is quite good for each of P or S wave data set. Both P and SH wave spectra have flat low frequency amplitudes and sharp corners. The values of a are obtained different between P and SH wave spectra. The resolution of parameter a , however, is poor, as is expected for a large value of a , and any value of a between 4 and 11 seems to fit P wave spectra. The high frequency decay rate γ , on the contrary, is determined accurately enough to distinguish average shapes of P and SH wave spectra.

In Fig. 10, Q values obtained for P and SH waves are plotted against frequency. The values of q and n are 360 ± 110 and 0.050 ± 0.091 for P waves, and 420 ± 230 and 0.114 ± 0.182 for SH waves, respectively. Vertical bars on the curves represent estimation errors of Q values at frequencies for which displacement spectra are measured.

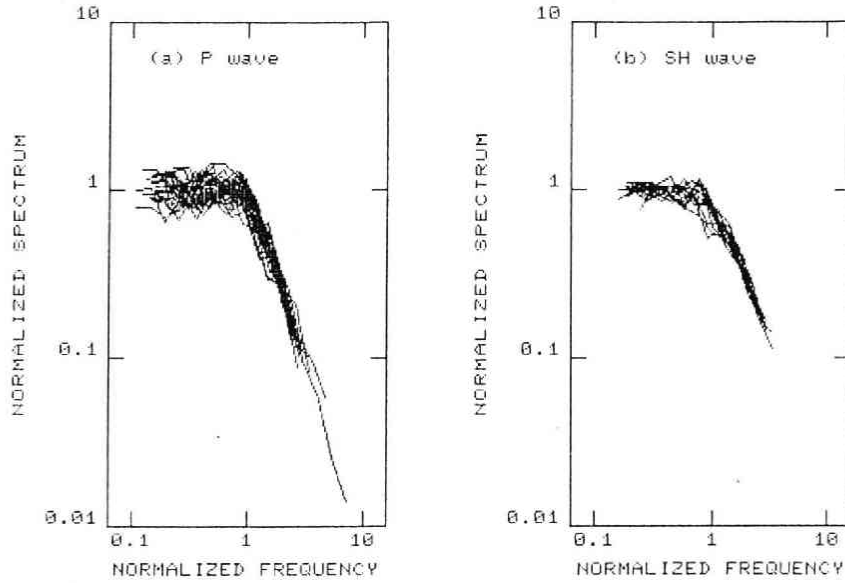


Fig. 9 Source displacement spectra of (a) P waves and (b) SH waves, whose amplitudes and frequency are normalized by the low frequency level and corner frequency, respectively. These diagrams visually verify the similarity in spectral shape both for P and SH waves.

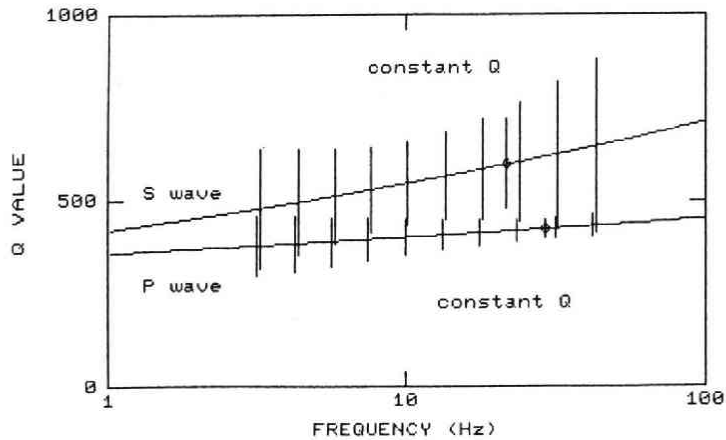


Fig. 10 Q values estimated for P and SH waves under the assumption of being frequency dependent as expressed in equation (5). Vertical bars indicate the probable errors in Q values at frequencies for which spectral measurements of the pulses were made. A circle and bar on each curve represent the comparative value of Q and its confidence limit as obtained under constant Q assumption.

Though the inversion procedure started with strongly frequency dependent Q values, the results show almost constant Q values both for P and SH waves. The Q value for P wave is about 380 at 3.2 Hz, and is 430 at 42 Hz. The Q value for SH wave is slightly more dependent on frequency. It takes a value of 480 at 3.2 Hz, and it slowly increases to a value of 640 at 42 Hz.

The solutions under constant Q constraint are also attempted from the same initial values and with the same damping constants to test the significance of frequency dependent model of Q . The results are listed in Table 3. The final data variances are 0.037 and 0.019 for P and SH wave data, respectively. These are quite the same with 0.037 and 0.019 in the case of frequency dependent Q . The values of constant Q are found to be 420 ± 30 for P wave and 610 ± 120 for SH wave, which are also plotted with error bars in Fig. 10 at frequencies where the curves for frequency dependent Q take the same values. High frequency decay rates γ are obtained as 1.98 ± 0.13 and 1.63 ± 0.22 , and values of a are 11.3 ± 5.1 and 4.30 ± 2.12 for P and SH waves, respectively. These parameters of spectral shape are similar to those obtained for the case of frequency dependent Q . Low frequency amplitudes and corner frequencies are also estimated as the same values as in the case of frequency dependent Q . All these mean that the data do not necessarily indicate frequency dependence of Q for P nor for SH waves.

5. Discussion

There have been difficulty in quantitative arguments about corner frequency shift. One of the reasons for difficulty is the lack of accuracy in measurements of corner frequencies, which arises from poor quality of data, inadequate correction for inelastic attenuation, and subjective technique to pick up corner frequencies. The present study provides a reliable result of corner frequency shift. The quality of data used in the analysis is quite good, and an objective inversion technique is employed to separate inelastic attenuation effect from spectra and to estimate corner frequencies of all earthquakes based on a universal standard. The corner frequencies of P and S waves are estimated accurately enough not only to show that P wave corners are higher than S wave corners but also to indicate that the average ratio is about 1.3 for the earthquakes. The inversion method also reveals the difference of high frequency fall-off between P and S waves.

The inversion technique used in the present study simultaneously determines Q value and source parameters, therefore the trade-off between Q value and high frequency fall-off must be carefully investigated. A check on the trade-off between Q value and high frequency fall-off may be done simply by examining the shapes of source spectra deduced from the observed ones by correction for inelastic attenuation. Since the source spectra have flat low frequency amplitudes, sharp corners, and definite high frequency fall-off, and the shapes of source spectra of all earthquakes are identical in spite of varieties of corner frequencies (Fig. 9), it is concluded that the attenuation effect is adequately removed from the observed spectra.

Another check on the trade-off is made by comparison of Q values with those

obtained in other studies. Umino and Hasegawa (1984) studied the three-dimensional structure of inelastic attenuation for S wave in the northeastern part of Honshu, Japan. Their results show that apparent Q value for S wave along the path of the present study is 500 to 600. Matsumoto (1987) also obtained Q structure in the northeastern part of Honshu, Japan, by analysing S wave codas. The value of Q was estimated as 400 at 12 Hz and as 710 at 24 Hz. Those values of Q from the previous studies in the northeastern part of Honshu are in good agreement with the present result of $Q \sim 600$ for S wave, though Q value in Matsumoto (1987) shows a strong dependence on frequency. The difference of behaviour of Q values against frequency may be due to the difference of path effects between direct S waves and coda waves. As discussed above, it is concluded that there is no trade-off between Q value and high frequency fall-off, and thus nor between Q value and corner frequency.

The Q value for P wave obtained in the present study is lower than that for S wave. The ratio of Q value for P wave to that of S wave is about 0.72. Anderson *et al.* (1965) obtained the ratio in the mantle of 2.25 for periods longer than 50 seconds using surface wave data. This ratio has widely been accepted and has been used in analyses of body waves at high frequencies (e.g., Umino and Hasegawa, 1984). Recently, lower Q values for P wave than those for S wave have been obtained in analyses of small earthquakes and at high frequencies (Aki and Chouet, 1975; Rautian *et al.*, 1978; Frankel, 1982; Butler *et al.*, 1987). There are many mechanisms likely to be responsible for attenuation of body waves (Jackson and Anderson, 1970) in each of frequency band from short to long periods. It is not known which mechanism is actually dominant in a particular band of frequency. The theoretical works by Savage (1966b) and Walsh (1966) predicted lower Q values of P waves than those of S waves, the ratio being from 0.3 to 0.6, which may be comparable with the ratio obtained here. This implies that S wave corner frequencies were correctly estimated, but not were underestimated. The ratio of P to S wave corner frequency is, therefore, considered reliable.

The ratio of P to S wave corner frequencies, together with the difference of high frequency fall-off between P and S waves, may place good constraints to admissible source models for earthquakes. A number of theoretical source models which have ever been proposed seem to be classified into two categories. One of them is represented by a long rectangular fault model with constant slip known as Haskell type model (Ben-Menahem, 1962; Haskell, 1964; Hirasawa and Stauder, 1964), and the other by an equidimensional or circular fault model (Savage, 1966a; Brune, 1970; Hanks and Wyss, 1972; Trifunac, 1972; Sato and Hirasawa, 1973; Madariaga, 1976; Masuda *et al.*, 1977). Theoretical studies have first been concentrated on searching explicit expressions of radiation fields in a closed form. The fault geometry, therefore, was mainly rectangular, and slip was assumed constant on the fault. As Hirasawa and Stauder (1965) pointed out, long fault models radiate S waves with narrower pulse widths than those of P waves to some particular directions. In other directions, S wave pulses may be broader than P wave pulses, but still the ratios are too small compared with most of the observed ratios. The theoretical predictions from long rectangular fault models seem

unfavourable to the majority of observations.

Savage (1966a), on the other hand, showed that longer S wave pulses are radiated from an elliptical or a circular fault, which is in favour of observations. Brune (1970) made a definite discussion on the corner of S wave displacement spectrum in relation to spatial extent of seismic source. Hanks and Wyss (1972) gave a relation between P wave corner frequency and source dimension by a simple replacement of S wave velocity with P wave velocity in Brune's relation. Thus the ratio of P to S wave corner frequency was presupposed to be 1.7. Trifunac (1972) followed the same way which Brune (1970) took in arguing the properties of S wave spectra, and derived a compatible relation between P wave corner frequency and source dimension. The ratio of P to S wave corner frequency was 1.46, which is different from the value assumed by Hanks and Wyss (1972), but is still greater than unity. Sato and Hirasawa (1973) discussed the corner frequency shift on the basis of a circular crack model of seismic source. P wave corner frequencies of their model were found always larger than S wave corners, though the ratios were dependent on directions of ray relative to the normal to fault. The models by Madariaga (1976) and by Masuda *et al.* (1977) were based on dynamical solutions to stress drops on fault surfaces. These models, as well as of Sato and Hirasawa (1973), predicted the average ratio of P wave corner frequency to S wave corner frequency as being 1.4 through 1.6. Compared with the model by Brune (1970), models by Sato and Hirasawa (1973), Madariaga (1976), and Masuda *et al.* (1977), which are in a sense based on more mathematical derivations, produce more complicated spectral shape near the corner.

It seemed that many observations of corner frequency shift preferred equidimensional or circular fault models to long rectangular fault models. Savage (1972), however, calculated far-field displacement spectra of P and S waves due to bilateral faulting on a rectangular surface to show that S wave corner frequencies are higher than P wave corner frequencies. Dahlen (1974) extended the theory to a general kinematic model of spontaneous nucleation of rupture with smooth healing, and reached a similar result of higher S wave corner frequency predicted by Savage (1972). The corner frequency analytically derived in Savage (1972) and Dahlen (1974) was defined as the frequency at which low and high frequency asymptotic trends intersect. According to the theory developed by Dahlen (1974), any source with smooth healing of fault motion must have higher corner frequency of S wave than that of P wave. This implies that corner frequency measurements in many of observations were incorrectly made by picking up wrong corners, or that measured corner frequencies were other corners than those defined as in Savage (1972) and in Dahlen (1974). The accurate estimation of corner frequency shift in the present study clearly indicates that the former is not likely. Savage (1974) also suggested that the latter is the case. It was shown in Savage (1974) that the spectrum has an intermediate frequency trend as well as high frequency asymptotic trend according to directions of radiation and to rupture velocity. It can be the case in an actual measurement that the second corner due to intermediate frequency trend would be taken as the corner due to high frequency trend, since frequency band

might not be wide enough to recognize high frequency asymptotic trend.

The high frequency trend termed and obtained in the present study is, in this sense, the intermediate frequency trend, and corner frequencies obtained here are the corners due to this intermediate frequency trend. The corner frequency as determined by graphical measurement in the literature (Molnar *et al.*, 1973; Sato and Hirasawa, 1973; Madariaga, 1976; Masuda *et al.*, 1977) also corresponds to the corner due to intermediate frequency trend rather than due to high frequency trend. Silver (1983) showed that the corner due to intermediate frequency trend matches better to the effective pulse width, which is closely related to temporal and spatial extent of seismic source. Silver (1983) also showed that the ratio of P to S wave corner frequency in those models is larger at larger angles to the fault normal and for the higher rupture velocity. The minimum ratio is 1.0 in the direction parallel to fault normal, and the maximum is about 1.4 through 1.6 in the direction perpendicular to fault normal for rupture velocity close to S wave velocity. The ratio of about 1.3 observed at the station location on the focal sphere suggests that possible sources responsible for the earthquakes analysed here are circular sources with rupture velocity close to S wave velocity. A unilateral rupture model would not account for the observed ratio, since the ratio predicted by the model is less than 1.2 (Savege, 1973; Silver, 1983). As shown in Sato and Hirasawa (1973), Madariaga (1976), and Masuda *et al.* (1977), the high frequency decay rate of S wave spectrum is more gradual than that of P wave spectrum for the rupture velocity close to S wave velocity. The difference of high frequency fall-off between P and S waves is, therefore, consistent with the model suggested by corner frequency ratio. A precise estimation of corner frequencies of P and S wave make it possible to estimate dynamical properties of seismic source as well as spatial extents of source. The high frequency fall-off of spectrum is also important for the study of source dynamics, though it was not always positively included in the previous studies.

6. Conclusions

By applying the objective inversion method developed by Masuda and Suzuki (1982), corner frequencies are accurately estimated for 34 P wave spectra and 14 SH wave spectra of small earthquakes. Although the observed spectra are the product of the source term and attenuation effect, the method successfully separates these two terms to expose the source spectra. The present study demonstrates that the inversion method used here is a strong tool for the studies of both source process and attenuation of seismic waves. The most important results are summarized in the followings:

(1) P wave corner frequencies are systematically higher than SH wave corner frequencies, the average ratio being about 1.3.

(2) High frequency fall-off of P wave spectrum, $f^{2.1}$, is faster than that of SH wave spectrum, $f^{1.7}$.

(3) The two results described above suggest that circular sources with rupture velocity close to S wave velocity are the case for the earthquakes studied here.

(4) Q values are nearly independent of frequency both for P and for S waves

throughout the frequency band between 3.2 to 42 Hz. The Q value for S wave is about 600, slightly higher than 430 for P wave.

Acknowledgments : I would like to thank Professors H. Hamaguchi, Z. Suzuki, and A. Takagi for suggestions throughout this study. I thank Professor Ohtake for helpful suggestions. I am deeply grateful to Professor T. Hirasawa for most valuable comments on the source theory. I am also grateful to Drs. A. Hasegawa and N. Umino for providing information about hypocenters and focal mechanisms of the earthquakes, and to the staff members of the Observation Center for Earthquake Prediction, Tohoku University for their help during the temporal observation at station MYK. I acknowledge the efforts of K. Saito and K. Ichikawa during the observation.

References

- Aki, K. and B. Chouet, 1975 : Origin of coda waves : Source, attenuation, and scattering effects, *J. Geophys. Res.*, 80, 3322-3342.
- Anderson, D.L., A. Ben-Menahem, and C.B. Archambeau, 1965 : Attenuation of seismic energy in the upper mantle, *J. Geophys. Res.*, 70, 1441-1448.
- Bakun, W.H., C.G. Bufe, and R.M. Stewart, 1976 : Body-wave spectra of Central California earthquakes, *Bull. Seism. Soc. Amer.*, 66, 363-384.
- Ben-Menahem, A., 1962 : Radiation of seismic body waves from a finite moving source in the Earth, *J. Geophys. Res.*, 67, 345-350.
- Brune, J.N., 1970 : Tectonic stress and the spectra of seismic shear waves from earthquakes, *J. Geophys. Res.*, 75, 4997-5009.
- Bungum, H., S. Vaage, and E.S. Husebye, 1982 : The Meloy earthquake sequence, Northern Norway : Source parameters and their scaling relations, *Bull. Seism. Soc. Amer.*, 72, 197-206.
- Butler, R., C.S. McCreery, L.N. Frazer, and D.A. Walker, 1987 : High-frequency seismic attenuation of oceanic P and S waves in the Western Pacific, *J. Geophys. Res.*, 92, 1383-1396.
- Dahlen, F.A., 1974 : On the ratio of P -wave to S -wave corner frequencies for shallow earthquake sources, *Bull. Seism. Soc. Amer.*, 64, 1159-1180.
- Fletcher, J.B., 1980 : Spectra from high-dynamic range digital recordings of Oroville, California aftershocks and their source parameters, *Bull. Seism. Soc. Amer.*, 70, 735-755.
- Frankel, A., 1982 : The effects of attenuation and site response on the spectra of microearthquakes in the northeastern Caribbean, *Bull. Seism. Soc. Amer.*, 72, 1379-1402.
- Hanks, T.C., 1981 : The corner frequency shift, earthquake source models, and Q , *Bull. Seism. Soc. Amer.*, 71, 597-612.
- Hanks, T.C. and M. Wyss, 1972 : The use of body-wave spectra in the determination of seismic-source parameters, *Bull. Seism. Soc. Amer.*, 62, 561-589.
- Hasegawa, H.S., 1983 : L_R spectra of local earthquakes recorded by the Eastern Canada telemetered network and spectral scaling, *Bull. Seism. Soc. Amer.*, 73, 1041-1061.
- Haskell, N.A., 1964 : Total energy and energy spectral density of elastic wave radiation from propagating faults, *Bull. Seism. Soc. Amer.*, 54, 1811-1841.
- Hirasawa, T. and W. Stauder, 1965 : On the seismic body waves from a finite moving source, *Bull. Seism. Soc. Amer.*, 55, 237-262.
- Jackson, D.D. and D.L. Anderson, 1970 : Physical mechanisms of seismic-wave attenuation, *Rev. Geophys. Space Phys.*, 8, 1-63.
- Madariaga, R., 1976 : Dynamics of an expanding circular fault, *Bull. Seism. Soc. Amer.*, 66, 639-666.
- Marion, G.E. and L.T. Long, 1980 : Microearthquake spectra in the Southeastern United States, *Bull. Seism. Soc. Amer.*, 70, 1037-1054.
- Masuda, T., 1982 : Scaling relations for source parameters of microearthquakes in the northeastern part of Japan, Doctor Thesis, Tohoku University.
- Masuda, T., S. Horiuchi and A. Takagi, 1977 : Far-field seismic radiation and its dependence upon

- the dynamic fracture process, Sci. Rep. Tohoku Univ. Ser. 5, Geophys., 24, 73-87.
- Masuda, T. and Z. Suzuki, 1982: Objective estimation of source parameters and local Q values by simultaneous inversion method, Phys. Earth Planet. Inter., 30, 197-208.
- Masuda, T. and A. Takagi, 1978: Source parameter estimates for small earthquakes, Sci. Rep. Tohoku Univ. Ser. 5, Geophys., 25, 39-54.
- Matsumoto, S., 1987: Coda Q structure in the northeastern part of Honshu, Japan, Master Thesis, Tohoku University.
- McGarr, A., R.W.E. Green, and S.M. Spottiswoode, 1981: Strong ground motion of mine tremors: Some implications for near-source ground motion parameters, Bull. Seism. Soc. Amer., 71, 295-319.
- Molnar, P., B.E. Tucker, and J.N. Brune, 1973: Corner frequencies of P and S waves and models of earthquake sources, Bull. Seism. Soc. Amer., 63, 2091-2104.
- Molnar, P. and M. Wyss, 1972: Moments, source dimensions and stress drops of shallow-focus earthquakes in the Tonga-Kermadec arc, Phys. Earth Planet. Inter., 6, 263-278.
- Peppin, W.A. and C.G. Bufe, 1980: Induced versus natural earthquakes: Search for a seismic discriminant, Bull. Seism. Soc. Amer., 70, 269-281.
- Rautian, T.G. and V.I. Khalturin, 1978: The use of the coda for determination of the earthquake source spectrum, Bull. Seism. Soc. Amer., 68, 923-948.
- Rautian, T.G., V.I. Khalturin, V.G. Martynov, and P. Molnar, 1978: Preliminary analysis of the spectral content of P and S waves from local earthquakes in the Garm, Tadjikistan region, Bull. Seism. Soc. Amer., 68, 949-971.
- Saito, K. and T. Masuda, 1981: Precursory change of spectral characteristics before the 1978 Miyagiken-oki earthquake, Sci. Rep. Tohoku Univ. Ser. 5, Geophys., 27, 95-109.
- Sato, H., 1986: Regional study of coda Q^{-1} in the Kanto-Tokai district, Japan, Zisin, Ser 2, 39, 241-249.
- Sato, T. and T. Hirasawa, 1973: Body wave spectra from propagating shear cracks, J. Phys. Earth., 21, 415-431.
- Savage, J.C., 1966a: Radiation from a realistic model of faulting, Bull. Seism. Soc. Amer., 56, 577-592.
- Savage, J.C., 1966b: Thermoelastic attenuation of elastic waves by cracks, J. Geophys. Res., 71, 3929-3938.
- Savage, J.C., 1972: Relation of corner frequency to fault dimensions, Bull. Seism. Soc. Amer., 77, 3788-3795.
- Savage, J.C., 1974: Relation between P - and S -wave corner frequencies in the seismic spectrum, Bull. Seism. Soc. Amer., 64, 1621-1627.
- Silver, P.G., 1983: Retrieval of source-extent parameters and the interpretation of corner frequency, Bull. Seism. Soc. Amer., 73, 1499-1511.
- Scherbaum, F. and D. Stoll, 1983: Source parameters and scaling laws of the 1978 Swabian Jura (Southwest Germany) aftershocks, Bull. Seism. Soc. Amer., 73, 1321-1343.
- Spottiswoode, S.M., and A. McGarr, 1975: Source parameters of tremors in a deep-level gold mine, Bull. Seism. Soc. Amer., 65, 93-112.
- Thatcher, W. and T.C. Hanks, 1973: Source parameters of Southern California earthquakes, Bull. Seism. Soc. Amer., 78, 8547-8576.
- Trifunac, M.D., 1972: Stress estimates for the San Fernando, California, earthquake of February 9, 1971: Main event and thirteen aftershocks, Bull. Seism. Soc. Amer., 62, 721-750.
- Umino, N. and A. Hasegawa, 1982: A detailed structure of the deep seismic zone and earthquake mechanism in the northeastern Japan arc, Zisin, Ser 2, 35, 237-257.
- Umino, N. and A. Hasegawa, 1984: Three-dimensional Q_s structure in the northeastern Japan arc, Zisin, Ser 2, 37, 217-228.
- Umino, N., A. Hasegawa, A. Takagi, S. Suzuki, Y. Motoya, S. Kameya, K. Tanaka, Y. Sawada, 1984: Focal mechanisms of intermediate-depth earthquakes beneath Hokkaido and Northern Honshu, Japan, Zisin, Ser 2, 37, 523-538.
- Walsh, J.B., 1966: Seismic wave attenuation in rock due to friction, J. Geophys. Res., 71, 2591-2599.

Appendix

The characteristic of band-pass filter at frequency f is expressed as,

$$\tilde{\theta}(f) = \frac{1}{1 + iQ_f(f/f_o - f_o/f)}, \quad (\text{A1})$$

f_o is the center frequency of pass band, and Q_f the quality factor of filter. If both amplitude and phase of input spectrum are almost constant within the effective pass band of filter, the output of filter is written as,

$$g(t) = |\tilde{v}(f_o)|\theta(t). \quad (\text{A2})$$

where $\tilde{v}(f_o)$ is Fourier amplitude spectrum of input signal at frequency f_o . The impulse response of filter $\theta(t)$ takes its maximum at $t=0$ and is given by,

$$\theta(t=0) = 2\pi f_o / Q_f. \quad (\text{A3})$$

Thus the following expression is valid:

$$|\tilde{v}(f_o)| = \frac{g_{\max}/2}{2\pi f_o / Q_f} \quad (\text{A4})$$

for maximum peak to peak amplitude of filter output g_{\max} and Fourier spectral component of frequency f_o . Equation (A4) is identical to equation (1) in section 2. If phase of spectrum changes by large amount, though amplitude of spectrum remains nearly constant, within a pass band of filter, the power of filter output is related to the power of input signal as,

$$\int |\tilde{g}(f)|^2 df = |\tilde{v}(f_o)|^2 \int |\tilde{\theta}(f)|^2 df. \quad (\text{A5})$$

The integral in the right hand side of equation (A5) is the power of impulse response of filter, and is calculated as,

$$\int |\tilde{\theta}(f)|^2 df = \pi f_o / Q_f. \quad (\text{A6})$$

The power of filter output may be approximately estimated as,

$$\int_0^{\tau_d} |g(t)|^2 dt = \frac{\tau_d (g_{\max}/2)^2}{2}, \quad (\text{A7})$$

where τ_d is the duration for which filter output retains an amplitude close to its maximum. From equations (A5) through (A7), an alternative relation is written as,

$$|\tilde{v}(f_o)| = \frac{g_{\max}/2}{\sqrt{2\pi f_o / Q_f \tau_d}}, \quad (\text{A8})$$

which is identical to equation (2) in section 2.

Masuda (1982) compared the spectra of P wave pulses of local earthquakes evaluated from filter outputs according to respective relations (A4) and (A8) with Fourier spectrum calculated by FFT algorithm. It is shown that at low frequencies where both amplitude and phase of spectrum are considered constant, spectral amplitude evaluated

from relation (A4) well represents amplitude of Fourier spectrum, while at high frequencies beyond a corner where phase of spectrum is no longer regarded as constant, amplitude according to equation (A8) fits better to Fourier spectrum than that due to equation (A4).